CRYSTAL GROWTH & DESIGN

pubs.acs.org/crystal

Article

Clamshell Arrangements and Chirality in Cocrystals of C_{70} with M^{II}(octaethylporphyrin) (M = Co or Zn)

Lilia M. Baldauf, James C. Fettinger, Marilyn M. Olmstead, Kamran B. Ghiassi, and Alan L. Balch*

Cite This: *Cryst. Growth Des.* 2023, 23, 915−922

Read Online

ACCESS | Metrics & More | Article Recommendations | Supporting Information

ABSTRACT: Two new cocrystals, $2C_{70}{\cdot}3Co^{II}(OEP){\cdot}2CHCl_3$ (**1**) (OEP is the dianion of octaethylporphyrin) and $C_{70}{\cdot}2Zn^{II}(OEP){\cdot}o$-xylene (**2**), with a clamshell arrangement of two porphyrins about a central C_{70} were grown and structurally characterized. The cocrystal $2C_{70}{\cdot}3Co^{II}(OEP){\cdot}2CHCl_3$ (**1**) possess a unique double-clamshell arrangement in which there are two distinct compartments for the fullerenes and a distorted $Co^{II}(OEP)$ molecule that is sandwiched between two C_{70} molecules. $C_{70}{\cdot}2Zn^{II}(OEP){\cdot}o$-xylene (**2**) has a simple clamshell arrangement of two $Zn^{II}(OEP)$ molecules surrounding the C_{70} molecule, with the clamshells arranged into chains through close face-to-face contacts between the porphyrins. In contrast, $C_{70}{\cdot}Zn^{II}(OEP){\cdot}1.5p$-xylene (**3**) has a more common structure with the C_{70} molecule in close proximity to only one $Zn^{II}(OEP)$ molecule.

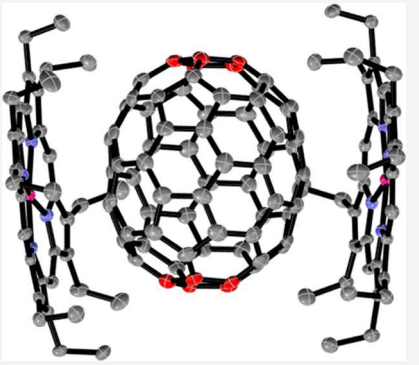

INTRODUCTION

Fullerenes are molecular allotropes of carbon that are distinguished by their solubilities in a range of organic solvents to produce colored solutions.[1,2] Fullerenes come in a variety of sizes and shapes.[3] The simplest cage, C_{60}, has a soccer ball shape with I_h symmetry. The next largest fullerene, C_{70}, however, has an oblong shape with D_{5h} symmetry and is the first in a series of fullerenes that are closely related to single-walled carbon nanotubes. Other members of this series that have been isolated and crystallographically characterized include $D_{5h}(1)$-C_{90}[4,5] and $D_{5d}(1)$-C_{100},[6,7] both with pentagonal end caps, and $D_{3d}(1)$-C_{96}[8,9] with hexagonal end caps. Fullerenes can also form isomers, and the number of possible isomers increases as the size of the fullerene increases. For example, in addition to $D_{5h}(1)$-C_{90}, two other C_{90} isomers of low symmetry, $C_1(30)$-C_{90} and $C_1(32)$-C_{90}, that are not nanotubular in shape have been crystallographically characterized.[10] For C_{96}, in addition to the nanotubular $D_{3d}(1)$-C_{96}, $C_2(181)$-C_{96} with a flat-sided, somewhat spherical shape has been identified crystallographically.[7] As these examples show, fullerenes have considerable diversity in their structures.

Determining the structure of a newly identified and isolated fullerene is a task that is best accomplished by single-crystal X-ray diffraction. However, the uniform surface of fullerenes with merely a collection of 12 pentagons and the appropriate number of hexagons frequently results in the formation of crystals that display significant disorder. Problems with disorder can frequently be overcome by cocrystallization of the fullerene or endohedral fullerene with a metalloporphyrin, usually $Ni^{II}(OEP)$ (OEP is the dianion of octaethylporphyrin).[11,12] This technique has been used to identify many new fullerenes[3,4,7,8] and endohedral fullerenes including cage isomers of endohedral fullerenes (e.g., $Er_2@C_s(6)$-C_{82},[13] $Er_2@C_{3v}(8)$-C_{82}[14]), endohedral fullerenes that violate the isolated pentagon rule (IPR) (e.g., $Gd_3N@C_s(51365)$-C_{84},[15] $Sc_3N@C_s(39663)$-C_{82}[16]), actinide endohedral fullerenes (e.g., $U@C_{82\text{-}86}$,[17] $Th_2@I_h(7)$-C_{80}[18]), endohedral fullerenes displaying single molecule magnetism (e.g., $TbNC@C_{2v}(19138)$-C_{76},[19] $Dy_2O@C_s(10528)$-C_{72}[20]), and large clusters within fullerene cages (e.g., $Sc_4C_2@I_h$-C_{80},[21] $Sc_4(\mu_3\text{-}O)_3@I_h$-$C_{80}$[22]).

In most cases where $Ni^{II}(OEP)$ cocrystallizes with a fullerene or endohedral fullerene, the asymmetric unit contains a 1:1 ratio of $Ni^{II}(OEP)$ and fullerene molecules with all eight ethyl arms of the porphyrin embracing the fullerene. However, we recently discovered that when C_{70} was allowed to cocrystallize with $Ni^{II}(OEP)$ in *p*-xylene solution, a remarkably complex crystal was obtained that contained 42 unique molecules in the asymmetric unit.[23] Figure 1 shows a drawing of the structure of $12Ni^{II}(OEP){\cdot}12C_{70}{\cdot}18p$-xylene at 90 K. The asymmetric unit contains 12 molecules of $Ni^{II}(OEP)$ that are paired with 12 molecules of C_{70} along with 18 molecules of *p*-xylene. The pairs of $Ni^{II}(OEP)$ and C_{70} molecules can be distinguished by the angle that the fivefold axis of the fullerene makes with the plane of the porphyrin. This angle varies from 0.3 to 9.7° in the 12 porphyrin/fullerene pairs.

Received: October 7, 2022
Revised: December 23, 2022
Published: January 9, 2023

https://doi.org/10.1021/acs.cgd.2c01136
Cryst. Growth Des. 2023, 23, 915−922

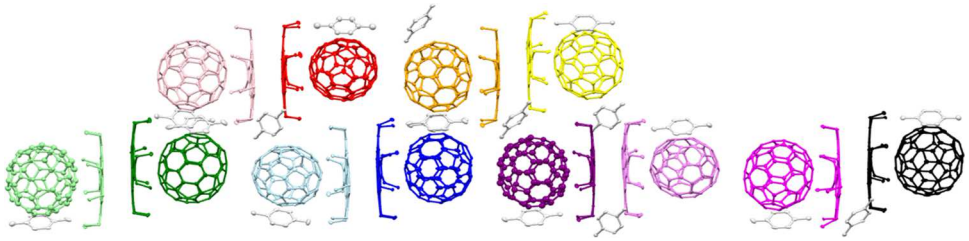

Figure 1. Asymmetric unit of $12Ni^{II}(OEP)\cdot12C_{70}\cdot18p$-xylene cocrystal at 90 K drawn from data in ref 23. Each C_{70} and $Ni^{II}(OEP)$ pair has a distinctive color. Thermal ellipsoids are drawn at 30%. Hydrogen atoms are omitted for clarity.

Table 1. Crystal Data for Cocrystals[a]

	$2C_{70}\cdot3Co^{II}(OEP)\cdot2CHCl_3$ (**1**)	$C_{70}\cdot2Zn^{II}(OEP)\cdot3o$-xylene (**2**)	$C_{70}\cdot Zn^{II}(OEP)\cdot1.5p$-xylene (**3**)
chemical formula	$C_{250}H_{134}N_{12}Cl_6Co_3$	$C_{166}H_{118}N_8Zn_2$	$C_{118}H_{59}N_4Zn$
formula weight	3695.17	2355.42	1598.06
radiation, λ (Å)	Cu ($K\alpha$)	Mo ($K\alpha$)	Mo ($K\alpha$)
crystal system	monoclinic	monoclinic	triclinic
space group	$P2_1$	$P2_1/n$	$P\bar{1}$
T (K)	100 (2)	90 (2)	90 (2)
a (Å)	14.9315 (5)	13.7400 (13)	15.2042 (10)
b (Å)	24.2226 (7)	27.584 (3)	15.9787 (11)
c (Å)	21.9933 (7)	30.402 (3)	16.5972 (11)
α (deg)	90	90	76.550 (3)
β (deg)	91.1506 (18)	101.499 (3)	72.160 (2)
γ (deg)	90	90	68.465 (2)
V (Å^3)	7952.9 (4)	9877	3537.3 (4)
Z	2	2	2
d_{calc}(Mg m^{-3})	1.543	1.386	1.486
μ (mm^{-1})	0.414	0.491	0.414
F(000)	3802	490	1650
crystal size, mm	0.284 × 0.281 × 0.202	0.480 × 0.240 × 0.060	0.092 × 0.030 × 0.024
reflections collected	239 537	62 454	138 166
data/restraints/parameters	51 895/1115/3158	20 878/162/1687	16 315/18/1107
R(int)	0.0681	0.820	0.0510
R_1 [data with $I > 2\sigma(I)$]	0.0660 (49 323)	0.0820 (10 532)	0.0427 (14 015)
wR_2 (all data)	0.1996	0.2452	0.1108
largest diff peak, hole (e Å^{-3})	1.889, −0.901	1.392, −1.064	0.654, −0.539

[a] $R_1 = \frac{\Sigma||F_o| - |F_c||}{\Sigma|F_o|}$; $wR_2 = \left\{\frac{\Sigma[w(F_o^2 - F_c^2)^2]}{\Sigma[w(F_o^2)^2]}\right\}^{1/2}$.

Recent systematic studies of the cocrystallization of C_{60} with the porphyrins $M^{II}(OEP)$ with (M = Co, Ni, Cu, and Zn) in a variety of solvents have shown that both the metal ion and the solvents play significant roles in determining the type of cocrystal formed, including the porphyrin/C_{60} stoichiometry and how the solids are organized.[24,25] Here, we explore whether C_{70} can form clamshell arrangements of two porphyrins around a single C_{70} molecule and complex cocrystals like $12Ni^{II}(OEP)\cdot12C_{70}\cdot18p$-xylene with other metal ions in the porphyrin and with other solvents.

RESULTS AND DISCUSSION

Cocrystal Growth. Crystals of $2C_{70}\cdot3Co^{II}(OEP)\cdot2CHCl_3$ (**1**), $C_{70}\cdot2Zn^{II}(OEP)\cdot o$-xylene (**2**), and $C_{70}\cdot Zn^{II}(OEP)\cdot p$-xylene (**3**) were prepared by layering a solution of C_{70} in chloroform, o-xylene, or p-xylene, respectively, over an equimolar solution of the appropriate $M^{II}(OEP)$ in an identical solvent. The reverse layering was also performed. Crystals began appearing within 3 days but were often left to grow for 2−4 weeks to reach the appropriate size for data collection. Crystallographic data for the crystals are shown in Table 1. Efforts to generate cocrystals of $Co^{II}(OEP)$ with C_{70} from solutions in o-xylene, p-xylene, or toluene were unsuccessful.

*Structure of $2C_{70}\cdot3Co^{II}(OEP)\cdot2CHCl_3$ (**1**).* The crystals form in the space group $P2_1$. The asymmetric unit contains two molecules of C_{70}, three molecules of $Co^{II}(OEP)$, and two disordered molecules of chloroform. The two molecules of C_{70} and three molecules of $Co^{II}(OEP)$ form a double-clamshell arrangement in which there are two compartments for the fullerenes. One of the C_{70} molecules is ordered, while the other is disordered and occupies two sites, the major site A with 0.58 occupancy and the minor site B with 0.42 occupancy. Figure 2 shows the asymmetric unit with the fivefold axis of each fullerene shown in a distinctive color. Part A of this figure was drawn showing the position of the major site for the disordered C_{70} molecule, while part B shows the location of the C_{70} molecule in the minor site.

The C_{70} and $Co^{II}(OEP)$ molecules are arranged into chains, as shown in Figure 3. The chloroform molecules (not shown) are not integrated within the chain but reside on the outer portion of the chain, similar to $12Ni^{II}(OEP)\cdot12C_{70}\cdot18p$-xylene[23] and $6Co^{II}(OEP)\cdot5C_{60}\cdot5CH_2Cl_2$.[24] Within the chain, there is a $Co^{II}(OEP)$ molecule that is sandwiched between two

https://doi.org/10.1021/acs.cgd.2c01136
Cryst. Growth Des. 2023, 23, 915−922

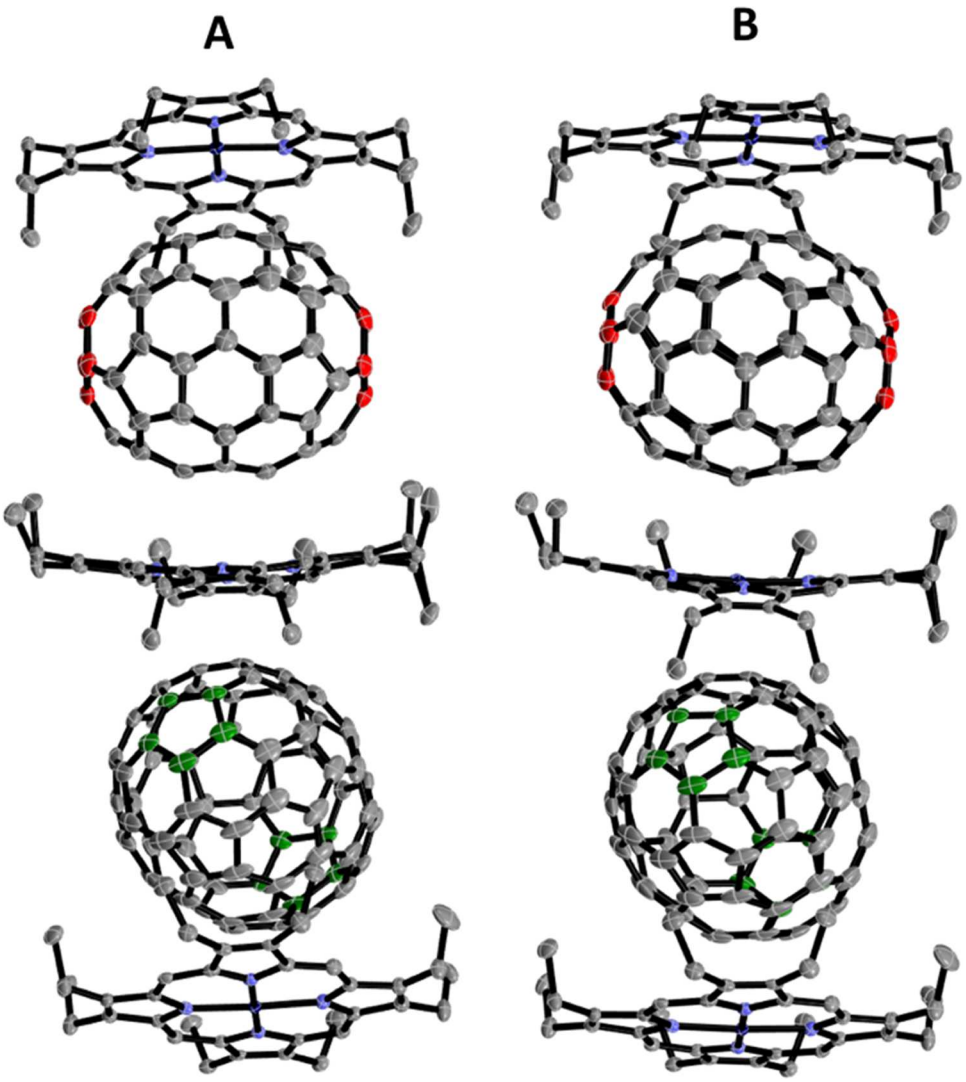

Figure 2. Asymmetric unit of $2C_{70}{\cdot}3Co^{II}(OEP){\cdot}2CHCl_3$ (**1**). The pentagons along the C_5 axis of the fullerene molecules are highlighted in red for the ordered site and green for the disordered site. Part A shows the asymmetric unit with the major orientation (0.58 occupancy) of the disordered C_{70} molecule, while B shows the same unit with the disordered C_{70} molecule in the minor (0.42 occupancy) site. Solvate molecules that reside on the sides of these chains and hydrogen atoms are omitted for clarity. Thermal ellipsoids are drawn at 50% probability.

C_{70} molecules, while the other two $Co^{II}(OEP)$ molecules make face-to-face contact between their planar portions. The $Co^{II}(OEP)$ molecule that is sandwiched between two C_{70} molecules has three of its ethyl groups embracing the ordered C_{70} molecule, while the remaining five ethyl groups hug the disordered C_{70} site. The other two $Co^{II}(OEP)$ molecules have all eight of their ethyl groups surrounding the adjacent C_{70} molecule. Notably, the structure of $2C_{70}{\cdot}3Co^{II}(OEP){\cdot}2CHCl_3$ (**1**) shows two interesting characteristics that are unique to C_{70} cocrystals: the adjustment of the C_{70} orientation to maximize the $\pi-\pi$ interactions between fullerene and porphyrin, and the distortion of the middle porphyrin to accommodate both fullerenes. Figure 3 also shows the packing in (**1**) highlighting the angles between the planar terminal $Co^{II}(OEP)$ molecules and the central $Co^{II}(OEP)$ molecule.

The orientation of the C_{70} molecule relative to the plane of the adjacent porphyrin can be quantified by considering the tilt angle, which is the angle between the C_5 axis of the C_{70} molecule and the plane of the porphyrin. As shown in Table 2, the C_{70} molecules generally have small tilt angles and are aligned nearly parallel to the plane of the neighboring porphyrin. However, the ordered C_{70} molecule in $2C_{70}{\cdot}3Co^{II}(OEP){\cdot}2CHCl_3$ (**2**) displays rather large tilt angles to both of the nearby porphyrins. These tilt angles have been seen in previous close-packed structures: fullerenes will offset themselves to maximize $\pi-\pi$ stacking from porphyrins.

Each crystal of $2C_{70}{\cdot}3Co^{II}(OEP){\cdot}2CHCl_3$ (**2**) is chiral since this material crystallizes in the Sohncke space group $P2_1$ with the component molecules packing about the 2_1 screw axis. However, the component molecules individually are not chiral. Similar formation of chiral crystals from achiral components occurs in other fullerene cocrystals, including the cocrystal of C_{70} with ferrocene ($C_{70}{\cdot}2(\eta^5\text{-}C_5H_5)_2$),[26] the cocrystal of C_{60} with hexamethylbenzene ($C_{60}{\cdot}C_6Me_6$),[27] and the cocrystal of tin tetraiodide with C_{60} ($C_{60}{\cdot}2SnI_4$).[28]

A unique feature of this structure is the distortion of the central porphyrin that is sandwiched between two fullerenes. In many other published fullerene/porphyrin cocrystals, it is more common for porphyrins to be stacked back-to-back, rather than situated between two fullerenes. For the C_{70} molecule, the flat planar portion of the molecule allows for better $\pi-\pi$ stacking with $M^{II}(OEP)$ than the spherical C_{60}

https://doi.org/10.1021/acs.cgd.2c01136
Cryst. Growth Des. 2023, 23, 915−922

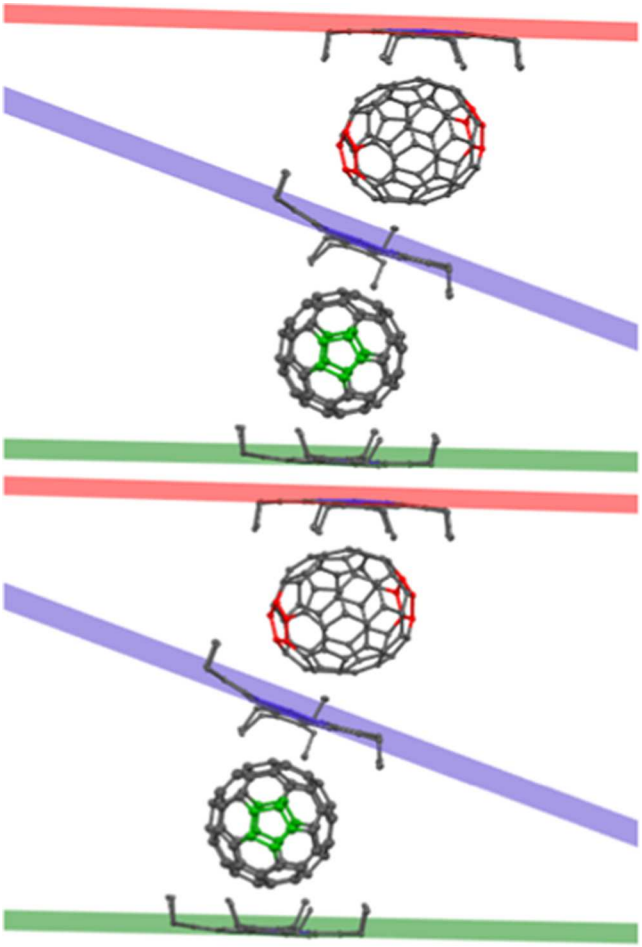

Figure 3. Chain structure of $2C_{70}{\cdot}3Co^{II}(OEP){\cdot}2CHCl_3$ (**1**) showing two asymmetric units. The C_5 axis of the fullerene molecules is highlighted in red and green to show the differences in fullerene orientation relative to the porphyrin. The orientation of the porphyrin planes is denoted by colored bars. Hydrogen atoms are omitted, and only the major orientation of the disordered C_{70} is shown.

molecule. This arrangement can result in more favorable fullerene−porphyrin interactions, where a porphyrin may be packed between two fullerenes, although this arrangement can cause some distortion in the central porphyrin.

This distortion of the porphyrin is best seen in the displacement plot shown in Figure 4, which allows a comparison of the central $Co^{II}(OEP)$ molecule of (**1**) to the other two $Co^{II}(OEP)$ molecules in that structure and to another cocrystal, $C_{70}{\cdot}Co^{II}(OEP){\cdot}C_6H_6{\cdot}CHCl_3$,[11] which has the more usual 1:1 $C_{70}/Co^{II}(OEP)$ stoichiometry. The central $Co^{II}(OEP)$ molecule in (**1**) is twisted into a saddle shape,[29] whereas the other $Co^{II}(OEP)$ molecules in that cocrystal display only very slight dome distortions. The distortion of the porphyrin and the disposition of the ethyl groups makes the $Co^{II}(OEP)$ chiral in this environment.

*Structure of $C_{70}{\cdot}2Zn^{II}(OEP){\cdot}3o$-xylene (**2**).* The asymmetric unit, which is shown in Figure 5, consists of a clamshell arrangement of two molecules of $Zn^{II}(OEP)$ and one molecule of C_{70} along with three molecules of *o*-xylene, two of which are disordered. All eight of the ethyl groups on each $Zn^{II}(OEP)$ molecule embrace the neighboring C_{70} molecule. The clamshell arrangement of two molecules of $Zn^{II}(OEP)$ and a C_{70} molecule are packed into chains as shown in Figure 5B. In these chains, pairs of $Zn^{II}(OEP)$ molecules make close back-to-back contact. Similar chains are seen in the clamshell structure of the C_{60} cocrystals, $C_{60}{\cdot}2M^{II}(OEP){\cdot}CHCl_3$, where M is Zn or Co.[25] The *o*-xylene molecules in $C_{70}{\cdot}2Zn^{II}(OEP){\cdot}3o$-xylene (**2**) reside in channels that run parallel to the chains formed by the $C_{70}{\cdot}2Zn^{II}(OEP)$ units as seen in the packing diagrams in Figure SI-2.

The porphyrins in $C_{70}{\cdot}2Zn^{II}(OEP){\cdot}3o$-xylene (**2**) have a slight dome distortion from planarity as can be seen in porphyrin displacement plots in Figure 6. As seen in Table 2, the tilt angles between the fivefold axis of the fullerene and the porphyrin planes are small, which allows $\pi-\pi$ overlap of the flat portion of the C_{70} molecule with the $Zn^{II}(OEP)$ molecule.

*Structure of $C_{70}{\cdot}Zn^{II}(OEP){\cdot}1.5p$-xylene (**3**).* Of the cocrystals reported here, $C_{70}{\cdot}Zn^{II}(OEP){\cdot}1.5p$-xylene (**3**) is the only one to have a common 1:1 $C_{70}/M^{II}(OEP)$ molar ratio. The asymmetric unit in (**3**) consists of an ordered C_{70} molecule, a $Zn^{II}(OEP)$ molecule, a disordered *p*-xylene molecule, and a half of another *p*-xylene molecule with the remaining half generated by a center of symmetry. Figure 7 shows a drawing of the interactions between the component molecules. As usual, the $Zn^{II}(OEP)$ molecule embraces the C_{70} molecule with all eight ethyl arms surrounding the fullerene. The tilt angle between the fullerene and porphyrin is small, 2.3°. The $Zn^{II}(OEP)$ molecule makes close face-to-face contact with another $Zn^{II}(OEP)$ molecule. One of the *p*-xylene molecules makes face-to-face contact with the C_{70} molecule. A packing diagram for $C_{70}{\cdot}Zn^{II}(OEP){\cdot}1.5p$-xylene (**3**) is shown in Figure

Table 2. Dimensions within Cocrystals

compound	tilt angle of C_5 axis of C_{70} from plane of the porphyrin (deg)	$C_{70}-Co^{II}(OEP)$ plane distance (Å)	metal−metal distance (Å)	porphyrin plane distances [nearest $Co^{II}(OEP)$] (Å)
$2C_{70}{\cdot}3Co^{II}(OEP){\cdot}2CHCl_3$ (**1**)			3.331	3.009
ordered site	31.2	6.314		
disordered site A	1.7	6.301		
disordered site B	3.0	6.301		
$2C_{70}{\cdot}3Co^{II}(OEP){\cdot}2CHCl_3$ (**1**) central $Co^{II}(OEP)$			12.795, 12.05	12.269, 12.651
ordered site	28.4	6.442		
disordered site A	1.6	6.357		
disordered site B	1.2	6.357		
$C_{70}{\cdot}2Zn^{II}(OEP){\cdot}3o$-xylene (**2**)	4.40, 4.90	3.072	3.185	3.446
$C_{70}{\cdot}Zn^{II}(OEP){\cdot}1.5p$-xylene (**3**)	2.30	3.047	3.131	N/A
$C_{70}{\cdot}Co^{II}(OEP){\cdot}$benzene$\cdot CHCl_3$	17.9	6.327	3.392	2.994

https://doi.org/10.1021/acs.cgd.2c01136
Cryst. Growth Des. 2023, 23, 915−922

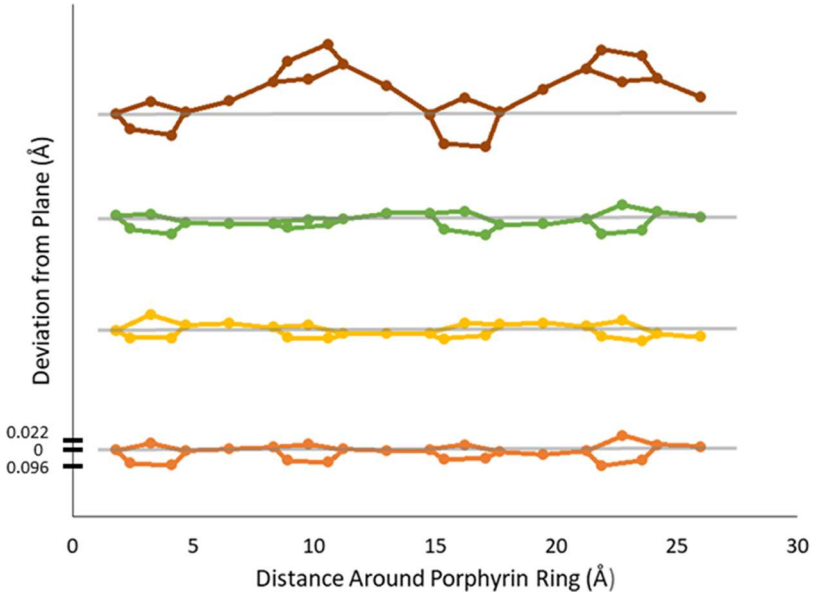

Figure 4. Porphyrin displacement plot showing out-of-plane distortion of the porphyrin core: deep red (top), central porphyrin plane of (**1**); green, terminal porphyrin of (**1**); yellow, terminal porphyrin of (**1**); light red (bottom), porphyrin plane of $C_{70}{\cdot}Co^{II}(OEP){\cdot}C_6H_6{\cdot}CHCl_3$.[11]

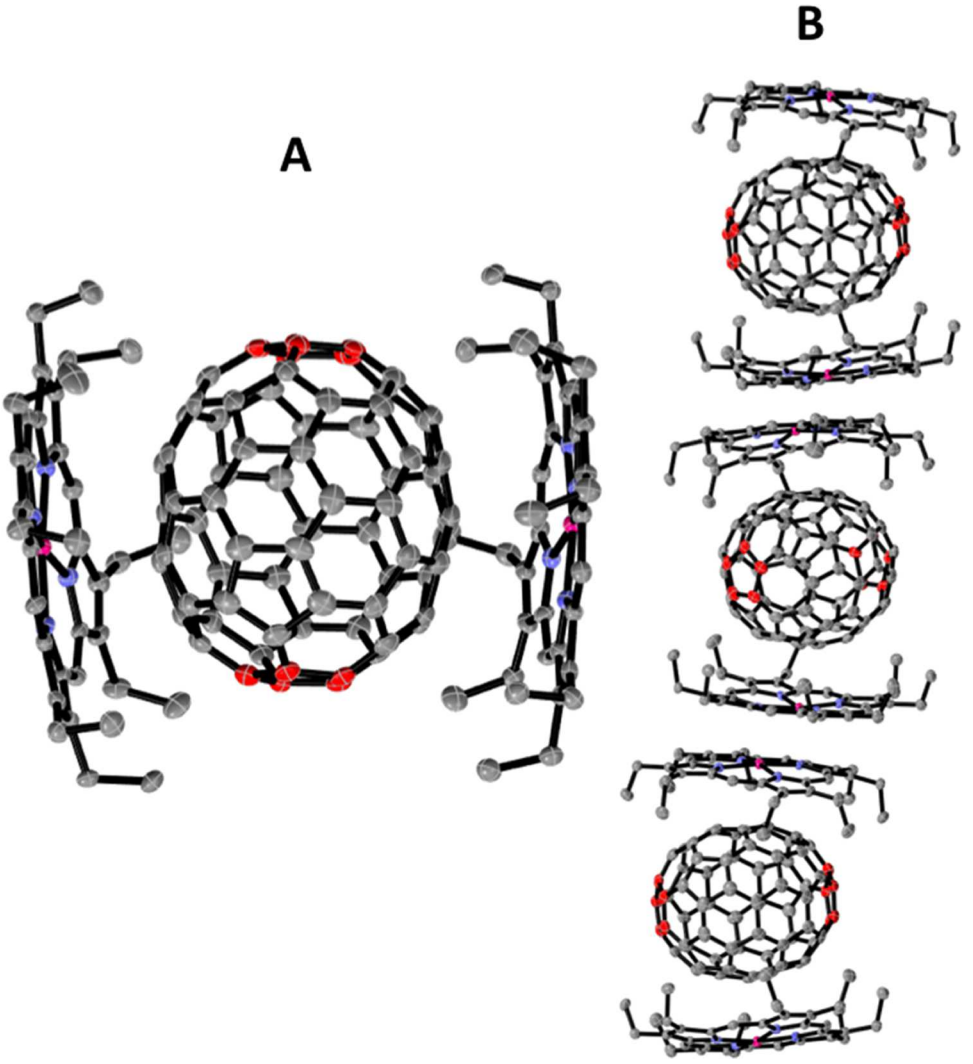

Figure 5. Asymmetric unit of $C_{70}{\cdot}2Zn^{II}(OEP){\cdot}3o$-xylene (**2**) (A) and a chain showing 3.66 asymmetric units (B). Solvent molecules that reside on the sides of these chains and hydrogen atoms were omitted for clarity. Thermal ellipsoids are shown at 50% probability.

https://doi.org/10.1021/acs.cgd.2c01136
Cryst. Growth Des. 2023, 23, 915−922

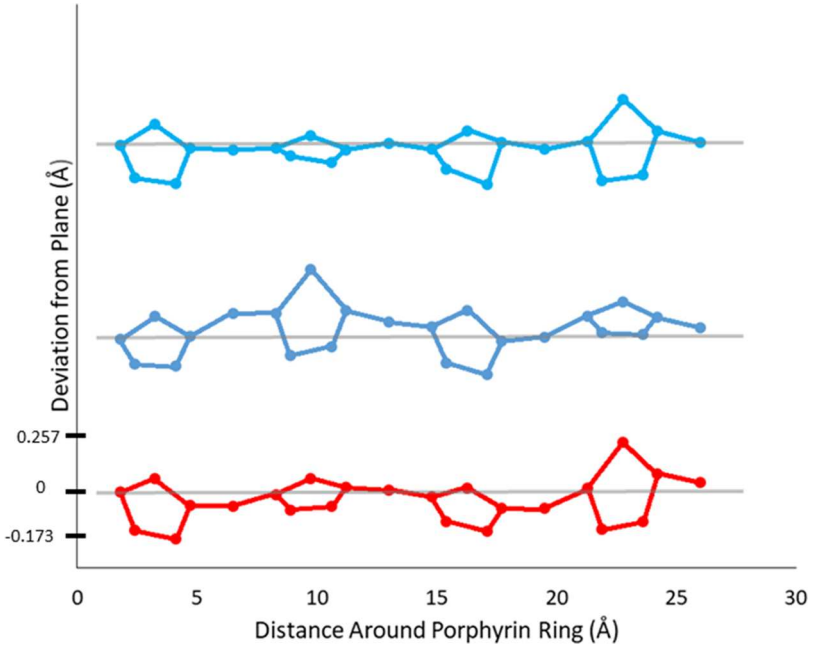

Figure 6. Porphyrin displacement plot showing the out-of-plane distortion of the porphyrin cores: blue and darker blue, Zn^{II}(OEP) porphyrin planes in (**2**); red, porphyrin plane in (**3**).

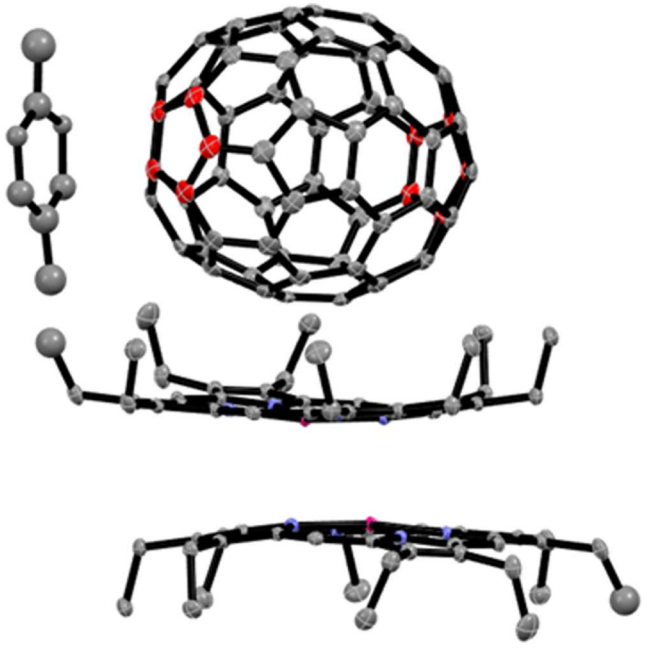

Figure 7. Structure of C_{70}·Zn^{II}(OEP)·1.5*p*-xylene (**3**) showing the C_{70}/Zn^{II}(OEP) and Zn^{II}(OEP)/Zn^{II}(OEP) interactions along with the major site of the disordered *p*-xylene molecule, which makes close contact with the fullerene. Hydrogen atoms were omitted for clarity. Thermal ellipsoids are drawn at 50% probability.

SI-3. C_{70}·Zn^{II}(OEP)·1.5*p*-xylene (**3**) is isostructural with C_{70}·Cu^{II}(OEP)·1.5*p*-xylene, whose structure was reported earlier.

CONCLUSIONS

Utilizing information gained in the studies of cocrystal formation of C_{60} and M^{II}(OEP),[11,24,25] two new cocrystals with a clamshell arrangement of two porphyrins about a central C_{70} were grown and structurally characterized. For C_{60}, the clamshell motif has been found only with Co^{II}(OEP) or Zn^{II}(OEP), but Ni^{II}(OEP) and Cu^{II}(OEP) have not been found to form the clamshell arrangement. Here, we have obtained the clamshell arrangement utilizing the same two metalloporphyrins. C_{70}·2Zn^{II}(OEP)·3*o*-xylene (**2**) has the usual clamshell arrangement seen in several cocrystals of C_{60} (e.g., C_{60}·2M^{II}(OEP)·$CHCl_3$, where M is Zn or Co),[11] while the structure of 2C_{70}·3Co^{II}(OEP)·2$CHCl_3$ (**1**) has a unique, double-clamshell arrangement of molecules. This double clamshell has two compartments for the C_{70} molecules and one Co^{II}(OEP) molecule that is sandwiched between the two fullerenes. While it is unusual to have such an arrangement, the nanotubular D_{5h}(1)-C_{90} forms the cocrystal D_{5h}(1)-C_{90}·Ni^{II}(OEP), which has chains of alternating D_{5h}(1)-C_{90} and Ni^{II}(OEP) molecules with Ni^{II}(OEP) molecules surrounded by two D_{5h}(1)-C_{90} molecules and the D_{5h}(1)-C_{90} molecules surrounded by two Ni^{II}(OEP) molecules. The tilt angle (3.2°) in this structure is small, and the central flat portion of the fullerene is situated above the porphyrin to maximize $\pi-\pi$ overlap. The porphyrin in D_{5h}(1)-C_{90}·Ni^{II}(OEP) is not nearly as distorted as is the central porphyrin in C_{70}·2Zn^{II}(OEP)·3*o*-xylene (**2**).

This study continues to demonstrate the important role of solvent in determining the stoichiometry and molecular organization within cocrystals of fullerenes and M^{II}(OEP). While the clamshell 2Zn^{II}(OEP)·*o*-xylene (**2**) crystallizes from *o*-xylene solution, changing the solvent to the isomeric *p*-xylene results in the formation of C_{70}·Zn^{II}(OEP)·1.5*p*-xylene (**3**) with the more common 1:1 C_{70}/M^{II}(OEP) stoichiometry. Prior work with C_{60} suggested that chlorinated solvents could produce crystals with unusual composition as was the case with the formation of 6Co^{II}(OEP)·5C_{60}·5CH_2Cl_2, 6Zn^{II}(OEP)·5C_{60}·5CH_2Cl_2, 6Co^{II}(OEP)·5C_{60}·5$C_2H_4Cl_2$, and 6Zn^{II}(OEP)·5C_{60}·5$C_2H_4Cl_2$.[24] Here, we utilized chloroform to form the unusual double clamshell, 2C_{70}·3Co^{II}(OEP)·2$CHCl_3$ (**1**). Also note that 2C_{70}·3Co^{II}(OEP)·2$CHCl_3$ (**1**) crystallizes from chloroform solution, but if a mixture of benzene and chloroform is used as the solvent, then a simple 1:1 cocrystal,

https://doi.org/10.1021/acs.cgd.2c01136
Cryst. Growth Des. 2023, 23, 915−922

C_{70}·Co^{II}(OEP)·C_6H_6·$CHCl_3$, forms.[11] We have been unable to find a situation that forms a cocrystal as complex as 12Ni^{II}(OEP)·12C_{70}·18*p*-xylene.

EXPERIMENTAL SECTION

Materials and General Consideration. H_2(OEP) was purchased from Frontier Scientific. Metalation of H_2(OEP) was accomplished by an established route.[30] C_{70} was purchased from SES Research with 99.5% purity. Solvents were obtained commercially and used as received.

Crystal Growth. *General Experimental Procedure.* In a clean scintillation vial, a solution of C_{70} in *p*-xylene (**1**), *o*-xylene (**2**), or chloroform (**4**) was prepared by sonication for approximately 20 min with a concentration of 1.5 mg/mL. In a separate scintillation vial, an equal concentration solution of M^{II}(OEP) in the identical solvent was prepared. Cocrystallization was conducted in sterile, thick-walled glass tubes with an approximate inner volume of 2.0 mL. A 1.0 mL portion of the M^{II}(OEP) solution was slowly pipetted into the tube through a filter pipet. Next, 1.0 mL of the C_{70} solution was carefully layered over the M^{II}(OEP) solution through a fresh filter pipet. For each combination of metalloporphyrins, additional tubes were prepared by the addition of the C_{70} solution to the tube with the subsequent addition of the M^{II}(OEP) solution. The crystal tubes were capped with a rubber septum and left undisturbed in dark cabinet until suitable crystal growth occurred.

Crystal Structure Determinations. Black blocks of C_{70}·2Zn^{II}(OEP)·3*o*-xylene (**2**) and C_{70}·Zn^{II}(OEP)·1.5*p*-xylene (**3**) were each mounted on a Bruker Apex II diffractometer employing a fine-focus Mo sealed tube (λ = 0.71073 Å). A black block of 2C_{70}·3Co^{II}(OEP)·2$CHCl_3$ (**1**) mounted in the 100 K nitrogen cold stream was provided by an Oxford Cryostream low-temperature apparatus on a Bruker Venture Kappa DUO diffractometer equipped with a molybdenum microsource (λ = 0.71073 Å). All data sets were reduced with the use of Bruker SAINT,[31] and a multiscan absorption correction was applied with the use of SADABS. Structure solutions and refinements were conducted with SHELXT-2015[32] and SHELXL-2018,[33] respectively. Crystallographic data are reported in Table 1.

ASSOCIATED CONTENT

Supporting Information

The Supporting Information is available free of charge at https://pubs.acs.org/doi/10.1021/acs.cgd.2c01136.

Packing diagrams for 2C_{70}·3Co^{II}(OEP)·2$CHCl_3$ (**1**) (Figures SI-1 and SI-2), C_{70}·2Zn^{II}(OEP)·3*o*-xylene (**2**) (Figures SI-3 and SI-4), and C_{70}·Zn^{II}(OEP)·1.5*p*-xylene (**3**) (Figure SI-5) (PDF)

Accession Codes

CCDC 2211098−2211100 contain the supplementary crystallographic data for this paper. These data can be obtained free of charge via www.ccdc.cam.ac.uk/data_request/cif, or by emailing data_request@ccdc.cam.ac.uk, or by contacting The Cambridge Crystallographic Data Centre, 12 Union Road, Cambridge CB2 1EZ, UK; fax: +44 1223 336033.

AUTHOR INFORMATION

Corresponding Author

Alan L. Balch − *Department of Chemistry, University of California, Davis, California 95616, United States;* orcid.org/0000-0002-8813-6281; Phone: (530) 752-0941; Email: albalch@ucdavis.edu; Fax: (530) 752-8995

Authors

Lilia M. Baldauf − *Department of Chemistry, University of California, Davis, California 95616, United States*

James C. Fettinger − *Department of Chemistry, University of California, Davis, California 95616, United States;* orcid.org/0000-0002-6428-4909

Marilyn M. Olmstead − *Department of Chemistry, University of California, Davis, California 95616, United States;* orcid.org/0000-0002-6160-1622

Kamran B. Ghiassi − *Air Force Research Laboratory, Aerospace Systems Directorate, Edwards AFB, California 93524, United States;* orcid.org/0000-0002-3557-2813

Complete contact information is available at: https://pubs.acs.org/10.1021/acs.cgd.2c01136

Notes

The authors declare no competing financial interest.

[§]Deceased.

ACKNOWLEDGMENTS

The authors thank the National Science Foundation for financial support (Grant CHE−1807637 to A.L.B. and M.M.O.). L.M.B. thanks the NSF-AGEP program and ARCS program for monetary support for this project.

REFERENCES

(1) Krätschmer, W.; Lamb, L. D.; Fostiropoulos, K.; Huffman, D. R. Solid C_{60}: a new form of carbon. *Nature* **1990**, *347*, 354−358.

(2) Georgakilas, V.; Perman, J. A.; Tucek, J.; Zboril, R. Broad Family of Carbon Nanoallotropes: Classification, Chemistry, and Applications of Fullerenes, Carbon Dots, Nanotubes, Graphene, Nanodiamonds, and Combined Superstructures. *Chem. Rev.* **2015**, *115*, 4744−4822.

(3) Fowler, P. W.; Manolopoulous, D. E.*An Atlas of Fullerenes*; Clarendon: Oxford, 1995.

(4) Yang, H.; Beavers, C. M.; Wang, Z. M.; Jiang, A.; Liu, Z. Y.; Jin, H. X.; Mercado, B. Q.; Olmstead, M. M.; Balch, A. L. Isolation of a Small Carbon Nanotube: The Surprising Appearance of $D_{5h}(1)$-C_{90}. *Angew. Chem.* **2010**, *122*, 898−902.

(5) Bowles, F. L.; Mercado, B. Q.; Ghiassi, K. B.; Chen, S. Y.; Olmstead, M. M.; Yang, H.; Liu, Z. Y.; Balch, A. L. Ordered Structures from Crystalline Carbon Disulfide Solvates of the Nanotubular Fullerenes $D_{5h}(1)$-C_{90} and D_{5h}-C_{70}. *Cryst. Growth Des.* **2013**, *13*, 4591−4598.

(6) Koenig, R. M.; Tian, H.-R.; Seeler, T. L.; Tepper, K. R.; Franklin, H. M.; Chen, Z.-C.; Xie, S.-Y.; Stevenson, S. Fullertubes: Cylindrical Carbon with Half-Fullerene End-Caps and Tubular Graphene Belts, Their Chemical Enrichment, Crystallography of Pristine C_{90}-$D_{5h}(1)$ and C_{100}-$D_{5d}(1)$ Fullertubes, and Isolation of C_{108}, C_{120}, C_{132}, and C_{156} Cages of Unknown Structures. *J. Am. Chem. Soc.* **2020**, *142*, 15614−15623.

(7) Stevenson, S.; Liu, X.; Sublett, D. M., Jr.; Koenig, R. M.; Seeler, T. L.; Tepper, K. R.; Franklin, H. M.; Wang, X.; Huang, R.; Feng, X.; Cover, K.; Troya, D.; Shanaiah, N.; Bodnar, R. J.; Dorn, H. C. Semiconducting and Metallic [5,5] Fullertube Nanowires: Characterization of Pristine $D_{5h}(1)$-C_{90} and $D_{5d}(1)$-C_{100}. *J. Am. Chem. Soc.* **2021**, *143*, 4593−4599.

(8) Yang, H.; Jin, H.; Che, Y.; Hong, B.; Liu, Z.; Gharamaleki, J. A.; Olmstead, M. M.; Balch, A. L. Isolation of four isomers of C_{96} and crystallographic characterization of nanotubular $D_{3d}(3)$-C_{96} and the somewhat flat-sided sphere $C_2(181)$-C_{96}. *Chem. - Eur. J.* **2012**, *18*, 2792−2796.

(9) Sanad, M. F.; Franklin, H. M.; Ali, B. A.; Puente Santiago, A. R.; Nair, A. N.; Chava, V. S. N.; Fernandez-Delgado, O.; Allam, N. K.; Stevenson, S.; Sreenivasan, S. T.; Echegoyen, L. Cylindrical C_{96} Fullertubes: A Highly Active Metal-Free O_2-Reduction Electrocatalyst. *Angew. Chem., Int. Ed.* **2022**, *61*, No. e202116727.

(10) Yang, H.; Mercado, B. Q.; Jin, H.; Wang, Z.; Jiang, A.; Liu, Z.; Beavers, C. M.; Olmstead, M. M.; Alan, L.; Balch, A. L. Fullerenes

without symmetry: crystallographic characterization of $C_1(30)$-C_{90} and $C_1(32)$-C_{90}. *Chem. Commun.* **2011**, *47*, 2068−2070.
(11) Olmstead, M. M.; Costa, D. A.; Maitra, K.; Noll, B. C.; Phillips, S. L.; Van Calcar, P. M.; Balch, A. L. Interaction of Curved and Flat Molecular Surfaces. The Structures of Crystalline Compounds Composed of Fullerene (C_{60}, $C_{60}O$, C_{70}, and $C_{120}O$) and Metal Octaethylporphyrin Units. *J. Am. Chem. Soc.* **1999**, *121*, 7090−7097.
(12) Stevenson, S.; Rice, G.; Glass, T.; Harich, K.; Cromer, F.; Jordan, M. R.; Craft, J.; Hadju, E.; Bible, R.; Olmstead, M. M.; Maitra, K.; Fisher, A. J.; Balch, A. L.; Dorn, H. C. Small-bandgap endohedral metallofullerenes in high yield and purity. *Nature* **1999**, *401*, 55−57.
(13) Olmstead, M. M.; de Bettencourt-Dias, A.; Stevenson, S.; Dorn, H. C.; Balch, A. L. Crystallographic Characterization of the Structure of the Endohedral Fullerene {$Er_2@C_{82}$ Isomer I} with C_s Cage Symmetry and Multiple Sites for Erbium along a Band of Ten Contiguous Hexagons. *J. Am. Chem. Soc.* **2002**, *124*, 4172−4173.
(14) Olmstead, M. M.; Lee, H. M.; Stevenson, S.; Dorn, H. C.; Balch, A. L. Crystallographic characterization of Isomer 2 of $Er_2@C_{82}$ and comparison with isomer 1 of $Er_2@C_{82}$. *Chem. Commun.* **2002**, 2688−2689.
(15) Zuo, T.; Walker, K.; Olmstead, M. M.; Melin, F.; Holloway, B. C.; Echegoyen, L.; Dorn, H. C.; Chaur, M. N.; Chancellor, C. J.; Beavers, C. M.; Balch, A. L.; Athans, A. J. New egg-shaped fullerenes: non-isolated pentagon structures of $Tm_3N@C_s(51365)$-C_{84} and $Gd_3N@C_s(51365)$-C_{84}. *Chem. Commun.* **2008**, 1067−1069.
(16) Guo, M.; Li, X.; Yao, Y.-R.; Zhuang, J.; Meng, O.; Yan, Y.; Liu, X.; Chen, N. A non-isolated pentagon rule C_{82} cage stabilized by a stretched Sc_3N cluster. *Chem. Commun.* **2021**, *57*, 4150−4153.
(17) Yao, Y.-R.; Roselló, Y.; Ma, L.; Santiago, A. R. P.; Metta-Magaña, A.; Chen, N.; Rodríguez-Fortea, A.; Poblet, J. M.; Luis Echegoyen, L. Crystallographic Characterization of $U@C_{2n}$ ($2n$ = 82−86): Insights about Metal−Cage Interactions for Mono-metallofullerenes. *J. Am. Chem. Soc.* **2021**, *143*, 15309−15318.
(18) Zhuang, J.; Morales-Martínez, R.; Zhang, J.; Wang, Y.; Yao, Y.-R.; Pei, C.; Rodríguez-Fortea, A.; Wang, S.; Echegoyen, L.; de Graaf, C.; Poblet, J. M.; Ning Chen, N. Characterization of a strong covalent Th^{3+}−Th^{3+} bond inside an $I_h(7)$-C_{80} fullerene cage. *Nat. Commun.* **2021**, *12*, No. 2372.
(19) Liu, F.; Wang, S.; Gao, C.-L.; Deng, Q.; Zhu, X.; Kostanyan, A.; Westerström, R.; Jin, F.; Xie, S.-Y.; Popov, A. A.; Greber, T.; Yang, S-F. Mononuclear Clusterfullerene Single-Molecule Magnet Containing Strained Fused-Pentagons Stabilized by a Nearly Linear Metal Cyanide Cluster. *Angew. Chem.* **2017**, *129*, 1856−1860.
(20) Velkos, G.; Yang, W.; Yao, Y.-R.; Sudarkova, S. M.; Liu, X. Y.; Büchner, B.; Avdoshenko, S. M.; Chen, N.; Popov, A. A. Shape-adaptive single-molecule magnetism and hysteresis up to 14 K in oxide clusterfullerenes $Dy_2O@C_{72}$ and $Dy_2O@C_{74}$ with fused pentagon pairs and flexible Dy−(μ_2-O)−Dy angle. *Chem. Sci.* **2020**, *11*, 4766−4772.
(21) Nie, M.; Meng, H.; Zhao, C.; Lu, Y.; Zhang, J.; Feng, L.; Wang, C.; Wang, T. Crystallographic evidence and spin activation for the Russian-doll-type metallofullerene $Sc_4C_2@C_{80}$. *Chem. Commun.* **2020**, *56*, 10879−10882.
(22) Mercado, B. Q.; Olmstead, M. M.; Beavers, C. M.; Easterling, M. L.; Stevenson, S.; Makay, M. A.; Coumbe, C. E.; Phillips, J. D.; Phillips, J. P.; Poblet, J. M.; Balch, A. L. A Seven Atom Cluster in a Carbon Cage, the Crystallographically Determined Structure of $Sc_4(\mu_3\text{-}O)_3@I_h$-$C_{80}$. *Chem. Commun.* **2010**, *46*, 279−281.
(23) Baldauf, L. M.; Ghiassi, K. B.; Olmstead, M. M.; Balch, A. L. Fullerene nanostructures: how the oblong shape of C_{70} forms a cocrystal with an enormous asymmetric unit and related cocrystals. *Nanoscale* **2020**, *12*, 20356−20363.
(24) Roy, M.; Olmstead, M. M.; Balch, A. L. Metal Ion Effects on Fullerene/Porphyrin Cocrystallization. *Cryst. Growth Des.* **2019**, *19*, 6743−6751.
(25) Roy, M.; Diaz Morillo, I. D.; Carroll, X. B.; Olmstead, M. M.; Balch, A. L. Solvent and Solvate Effects on the Cocrystallization of C_{60} with Co^{II}(OEP) or Zn^{II}(OEP) (OEP = Octaethylporphyrin). *Cryst. Growth Des.* **2020**, *20*, 5596−5609.
(26) Olmstead, M. M.; Hao, L.; Balch, A. L. Organometallic C_{70} chemistry. Preparation and crystallographic studies of (η^2-C_{70})Pd-(PPh_3)$_2$ · CH_2Cl_2 and (C_{70}) · 2{(η^5-C_5H_5)$_2$Fe}. *J. Organomet. Chem.* **1999**, *578*, 85−90.
(27) Domrachev, G. A.; Shevelev, Y. A.; Cherkasov, V. K.; Fukin, G. K.; Markin, G. V.; Kirillov, A. I. Fullerene complexes with bis($\eta^{\square}$-hexamethylbenzene)chromium, hexamethylbenzene, and hexaethylbenzene. *Russ. Chem. Bull.* **2006**, *55*, 225−229.
(28) Straus, D. B.; Cava, R. J. Self-Assembly of a Chiral Cubic Three-Connected Net from the High Symmetry Molecules C_{60} and SnI_4. *J. Am. Chem. Soc.* **2020**, *142*, 13155−13161.
(29) Ishizuka, T.; Grover, N.; Kingsbury, C. J.; Kotani, H.; Senge, M. O.; Kojima, T. Nonplanar porphyrins: synthesis, properties, and unique functionalities. *Chem. Soc. Rev.* **2022**, *51*, 7560−7630.
(30) Asano, M.; Kaizu, Y.; Kobayashi, H. The lowest excited states of copper porphyrins. *J. Chem. Phys.* **1988**, *89*, 6567−6576.
(31) Bruker, A. X. S.*SAINT and SADABS*; Bruker AXS Inc.: Madison, WI, 2018.
(32) Sheldrick, G. M. SHELXT - Integrated space-group and crystal-structure determination. *Acta Crystallogr., Sect. A: Found. Adv.* **2015**, *71*, 3−8.
(33) Sheldrick, G. M. Crystal structure refinement with SHELXL. *Acta Crystallogr., Sect. C: Struct. Chem.* **2015**, *71*, 3−8.

https://doi.org/10.1021/acs.cgd.2c01136
Cryst. Growth Des. 2023, 23, 915−922